

Supported lipid bilayer microarrays created by non-contact printing

Stefan Kaufmann* Jens Sobek† Marcus Textor‡
Erik Reimhult§

April 10, 2011

Electronic Supplementary Information

Buffer film thickness

The influence of the buffer film thickness on the dispensing process was investigated by using different buffer volumes to wet the clean, hydrophilic glass slide. A buffer thickness of $\approx 90 - 180 \mu\text{m}$ was proven to be suitable for the dispensing process whereas a thickness of $\approx 270 \mu\text{m}$ did not result in fluid SLBs, but only in adsorbed vesicles as seen in Figure S 1. The low adsorption of vesicles and lack of SLB formation for buffer films of $270 \mu\text{m}$ thickness is likely due to that the dispensed droplet does not fully penetrate down to the substrate surface. The resulting lower concentration close to the substrate surface combined with dilution through diffusion leads to low adsorption. Below a buffer film thickness of $\approx 90 \mu\text{m}$ evaporation of the water film was too fast for the dispensing process and protection of the vesicle solutions from drying could not be assured.

*Laboratory for Surface Science and Technology, Department of Materials, ETH Zurich, Switzerland

†Functional Genomics Center Zurich, Switzerland

‡Laboratory for Surface Science and Technology, Department of Materials, ETH Zurich, Switzerland

§Department of Nanobiotechnology University of Natural Resources and Life Sciences Vienna, Vienna, Austria E-mail: erik.reimhult@boku.ac.at

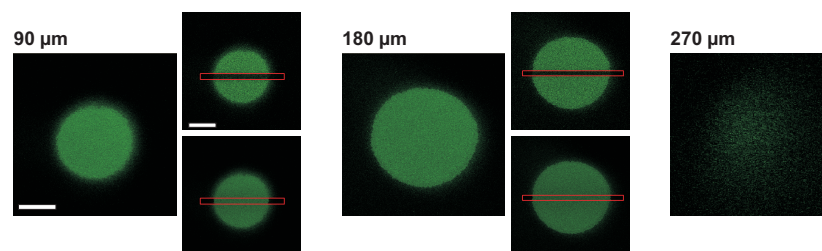


Figure S 1: The images show SLB formation in the case of buffer film thicknesses of 90 and 180 μm and low density of vesicle adsorption for 270 μm thick buffer films. (Dispensing: 5 droplets per spot, 3 min incubation). FRAP was used to confirm the presence of SLBs for 90 and 180 μm (shown as smaller images at the right of the respective image). Scalebar: 100 μm .

Rinsing artifacts

Figure S 2 shows two spots that have tail artifacts due to insufficiently fast rinsing with sufficient volume. The tails contain adsorbed vesicles or SLB patches which are not connected to the main spot. This lipid material was likely transported to the tail area by the rinsing flow.

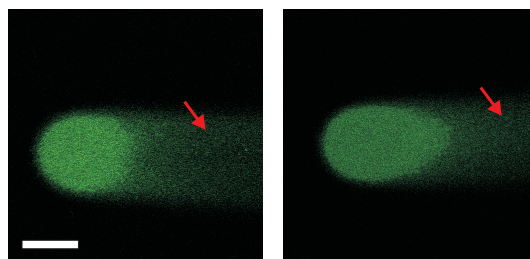


Figure S 2: Microscopy images of spots that show a tail artifact caused by inadequate rinsing (1 dispensed droplet with 3 minutes incubation time). Scalebar: 100 μm .

Estimation of vesicle layer at edge of spots

To estimate the dimension of the vesicle layer at the edge of the SLB spot, images before the bleach cycle (pre-bleach) and images after fluorescence recovery (post-bleach) of FRAP sequences were analysed. ImageJ¹ was used to subtract post-bleach from prebleach images with the result presented in Figure S3. In the subtraction images the area containing vesicles (non-recovered fluorescence) is observed as a slightly brighter

region at the edge of the spot indicated by red bars. For 1, 5, 10, 15 and 20× dispensed droplets (3 minutes incubation, 1 mg/ml vesicle solution) this region is indicated with a red scalebar in Figure S3. The dimension of the vesicle containing boundary region is extending from approximately maximally 5 μm (1×) to 35 μm (15×) for spot sizes ranging from 180 - 360 μm and is dependent on the number of dispensed droplets and on the rinsing procedure as shown in Figure S2. We emphasize that also planar lipid membrane islands might be present in this region since already at a vesicle surface coverage of $\approx 30\%$ unconnected planar membrane islands will occur.² Unconnected membrane islands will also lead to no recovery of fluorescence during FRAP measurements.

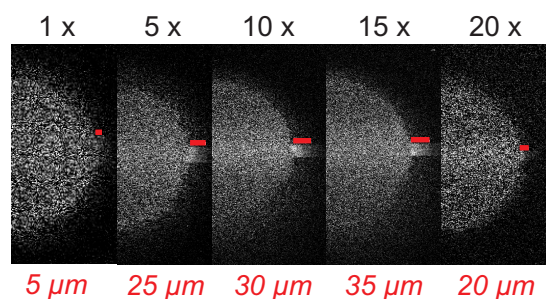


Figure S 3: FRAP images with post-bleach frames subtracted from pre-bleach frames. Spots with 1, 5, 10, 15 and 20× dispensed droplets, 3 minutes incubation and 1 mg/ml spotting solution are shown.

Interruption of SLB formation by early rinsing

Figure S 4 presents a FRAP measurement of a single dispensed droplet with an incubation time of 10 seconds. The small recovered area in the middle of the spot indicates that the SLB formation did not proceed to completion. The SLB is surrounded by a ring of adsorbed vesicles, indicating that SLB formation proceeds from the center and outwards. Figure S 4 is an addendum to Figure 2 in the main article which shows the evolution of the spot with longer incubation time.

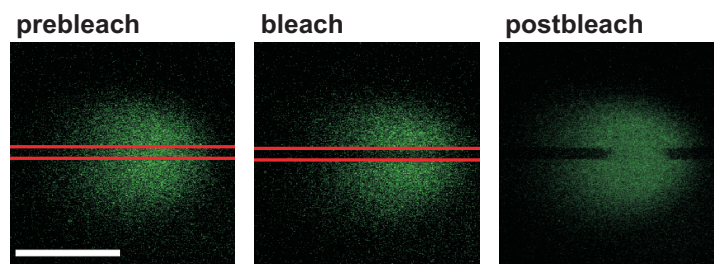


Figure S 4: FRAP measurement of a spot after dispensing 1 droplet and incubation for 10 seconds. The pre-bleach image shows a diffuse spot with adsorbed vesicles. Bleaching of a rectangular pattern revealed a small SLB in the center of the adsorbed vesicle spot. Both vesicle adsorption and SLB formation starts from the center and proceeds outwards. Scalebar 100 μm .

Flexibility of spotting method with an example of supported polymer-lipid bilayers

The flexibility of the presented spotting method allows the formation also of slow-forming SLBs³ from vesicles comprising POPC lipids mixed with PEG-lipids. The PEG-vesicles containing (1,2-dioleoyl-*sn*-glycero-3-phosphoethanolamine-N-[methoxy-(polyethylene glycol)-5000]) (PEG(5000)-PE) or (1,2-dioleoyl-*sn*-glycero-3-phosphoethanolamine-N-[methoxy-(polyethylene glycol)-2000]) (PEG(2000)-PE) were used with 20 mM EDTA (Sigma-Aldrich Buchs, Switzerland) added to the buffer just before conducting the measurements to speed up the formation process⁴. Measurements or rinsing steps were conducted with TBS. Figure S 5 shows FRAP images of a spot produced by dispensing 1 droplet of 0.5 mol% PEG(5000)-PE and 6 mol% PEG(2000)-PE with 3 minutes of incubation time.

Intermixing of SLB spot with additionally injected vesicles

The two movies show the fusion of a NBD-PC labeled spot with a subsequently forming SLB with Rhodamine labeled vesicles as presented in Figure 4 in the main article. Movie 1 presents the channel of the NBD-PC labels showing the fusion of the NBD-PC labels with Rhodamine labeled lipids and the dilution of the NBD-PC labels. Movie 2 shows the channel of the Rhodamine labeled lipids where they adsorb at the edge of the

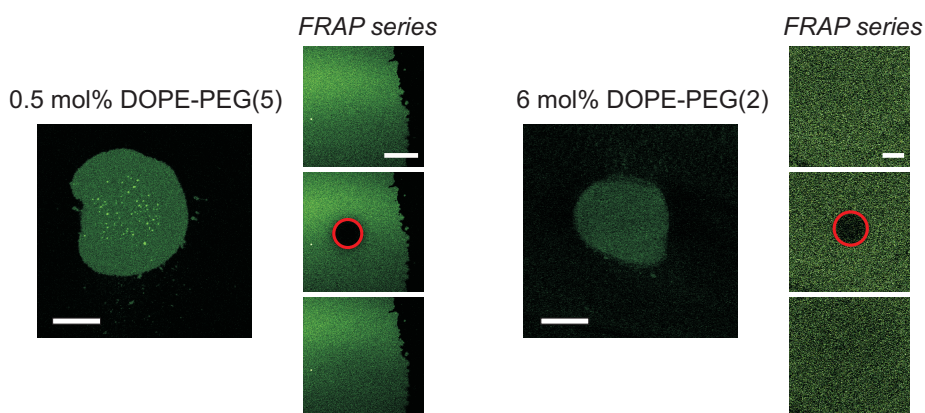


Figure S 5: SLB spots formed from vesicles with 0.5 mol% DOPE-PEG(5) and 6 mol% DOPE-PEG(2) mixed with POPC are shown. (Dispensing: 1 droplet, 3 minutes incubation.) Scalebar: 100 μm (FRAP series: scalebar: 20 μm).

NBD-PC labeled spot and start to dilute the NBD-PC labels from the spot, resulting in a homogeneous Rhodamine-labeled SLB. Images were taken each minute and the size of the images are 450 \times 450 μm .

Initial conditions for the calculated of spot sizes

Figure S 6 shows the effect of changing the initial vesicle distribution on the calculated time evolution. The starting time t_0 , as described in the Experimental section, was chosen such that i) $r = 45 \mu\text{m}$ and 99.9 % of all vesicles are deposited within this r and, ii) $r = 80 \mu\text{m}$, and 99.9 % and iii) $r = 45 \mu\text{m}$ and 80% respectively. These starting conditions were chosen since the droplet has approximately a radius of 45 μm and it is assumed that the lipid material is mostly confined within this radius following the Gaussian distribution of $s(r)$ after deposition of a droplet leading to conditions i) and iii). The average spot radius of spots on a dry glass slide was measured to be 80 μm which provides a maximum estimation of the original area over which lipid material is distributed at $t = 0 \text{ s}$ leading to condition ii). It is evident that the chosen starting conditions for the calculation influence the spot size at the beginning, indicated by a relative increase of the radii by a factor of 1.53 - 2.00 for conditions ii) and iii) with respect to condition i) which was used in the main text. The difference disappears for

longer incubation times and after 20 minutes all three conditions result in the same spot radius.

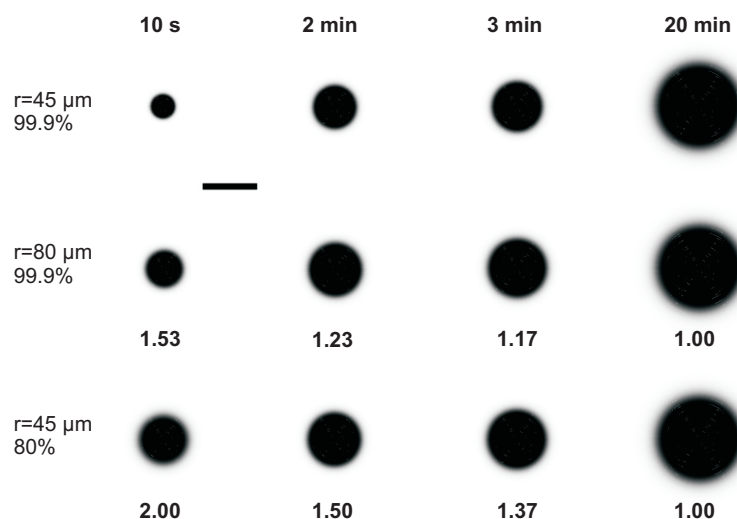


Figure S 6: Dependence of the spot evolution on the chosen initial conditions. The initial conditions are given for each row at the beginning of the sequence of the calculated spot sizes. In the main text condition i) with $r=45\ \mu\text{m}$ and 99.9 % was used. The numbers below the spots indicate the relative increase of the radius with reference to condition i) used in the main article. Scalebar 200 μm .

Time evolution of the spot size for multiple dispensed droplets

Figure S 7 shows the theoretical spot sizes obtained from the simulation and the experimental spot sizes for repeated droplet dispensing. Spots with 5, 10, 15 and 20 dispensed droplets are shown after 3 and 20 min of incubation. The first row in each case presents measured and the second row calculated spot sizes. The selection of the initial conditions in these cases is not straightforward since it is not known how the lipid material is distributed within the thin buffer film. It is assumed that due to the repeated dispensing the material is spread to a certain extent by convection during multiple droplet impact. As an approximation the spot sizes that were dispensed on a dry glass slide could again provide a basis for the estimation. The following values were chosen based on these results: $r=71\ \mu\text{m}$ (5 \times), $r=92.5\ \mu\text{m}$ (10 \times), $r=109.5\ \mu\text{m}$ (15 \times), $r=121\ \mu\text{m}$ (20 \times) where again 99.9 % of the total lipid material was assumed to be deposited within the volume

defined by this area and were shown as can be seen in Figure S6 to be reasonable approximations of the initial vesicle distribution. The comparison demonstrates that the experimental spot sizes also for repeated droplet dispensing do not show a considerable increase in size with increasing incubation time whereas the simulation predicts an observable size increase.

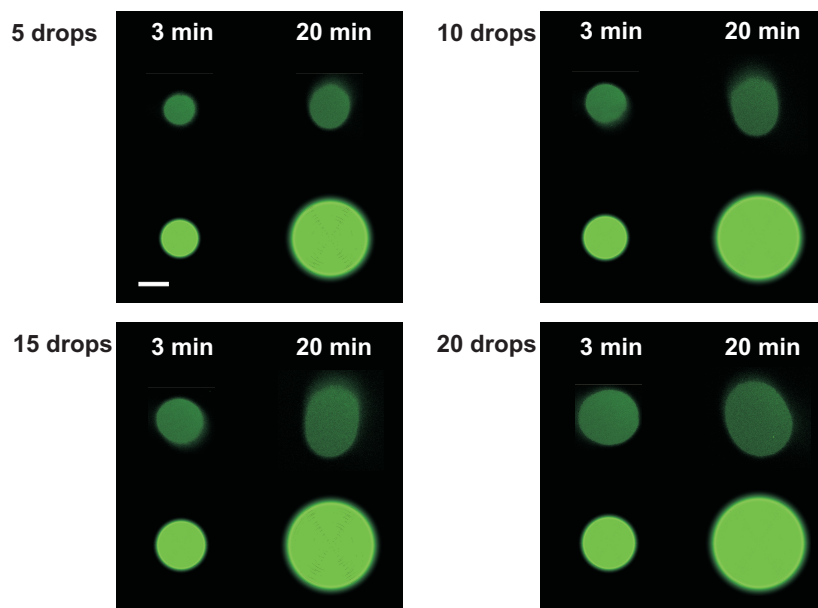


Figure S 7: Spot sizes of 5×, 10×, 15×, 20× droplets dispensing. The figure shows the spot size of the measured spots after 3 and 20 minutes (first row) and the calculated spot sizes (lower row). Scalebar 200 μm.

Calculation of the depletion zone at the air-buffer interface

To estimate the growth of the depletion zone at the air-buffer interface to a depth at which the adsorption of vesicles to the glass substrate is significantly affected, we calculate the diffusion length. If we equal this diffusion length with the total buffer film thickness, we can calculate the characteristic time which is needed to form a depletion zone with the dimension of the buffer film thickness.

For one-dimensional diffusion along the z -axis orthogonal to the interface, a step function profile is assumed for the initial condition, see Eq. 1. The initial condition determines the homogeneous initial concentration $c_{-\infty}$ at $z < 0$ and c_{∞} at $z > 0$. The

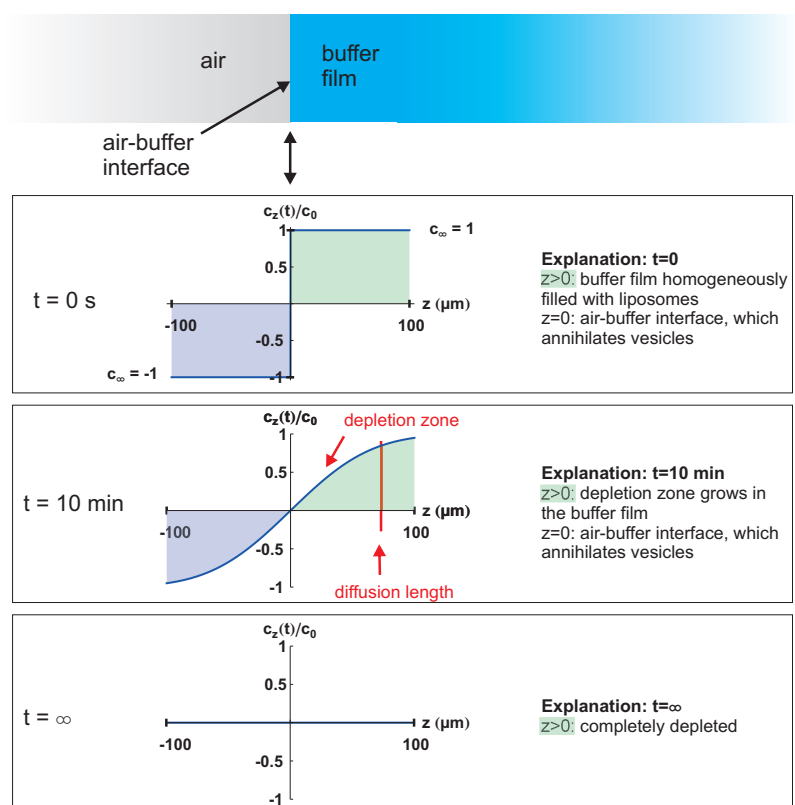


Figure S 8: The build-up of a depletion zone for the concentration $c_{-\infty} = -1$ and $c_{\infty} = 1$ is shown, where the right hand side is homogeneously filled with vesicles ($t = 0$). These vesicles are constantly annihilated at the air-buffer interface ($z = 0$), which is resulting in a depletion zone at the air-buffer interface for $t > 0$, e.g. $t = 10 \text{ min}$. After an infinite waiting time, all vesicles are annihilated and the concentration in the inspected distance range drops to $c \approx 0$, i.e. the buffer film is completely depleted.

solution to the diffusion equation with the initial conditions in Eq. 1 can be found in various textbooks and is given by the error function in Eq. 3 with D the vesicle bulk diffusion coefficient. Figure S 8 illustrates the initial concentration step function at $t = 0$ and the temporal evolution of the concentration with the formation of the depletion zone.

$$c(z, t = 0) = \begin{cases} c_{-\infty} & -\infty < z < 0 \\ c_{\infty} & 0 < z < \infty \end{cases} \quad (1)$$

$$c(-\infty, t) = c_{-\infty}$$

$$c(\infty, t) = c_{\infty}$$

(2)

$$c(z, t) = \frac{c_{-\infty} + c_{\infty}}{2} - \frac{c_{-\infty} - c_{\infty}}{2} \operatorname{erf}\left(\frac{z}{2\sqrt{Dt}}\right) \quad (3)$$

The depletion zone at the air-buffer interface is estimated by the diffusion length and the corresponding time which is needed to form a depletion zone with the dimension of the buffer film thickness. The diffusion length is defined as $d_p = 2\sqrt{Dt}$. Choosing $d_p = 88 \mu\text{m}$ corresponding to the buffer film thickness for the experimental conditions and $D = 2.18 \cdot 10^{-12} \text{ m}^2/\text{s}$ calculated from the Einstein-Stokes equation for the used vesicle size results in a characteristic time of $t_c = 888 \text{ s} \approx 15 \text{ min}$. With the characteristic time of $t_c \approx 15 \text{ min}$ a decrease in the vesicle concentration to 52% of the initial value is occurring in the center of the buffer film and to 84% of the initial concentration at the surface of the substrate ($z = 88 \mu\text{m}$). This first order estimate thus predicts significant influence from lipid loss at the air-buffer interface.

Another probable contributing process is the capture of lipids at the air-buffer interface of the dispensed droplet, corresponding to a vesicle loss of 13.4 %¹ with a lipid concentration of 1 mg/ml.

¹With a droplet radius of $r_{\text{droplet}} = 45 \mu\text{m}$, the number of vesicles captured at the surface of the droplet would approximately be $\frac{1}{2} \left[4\pi r_{\text{droplet}}^2 / (4\pi r_{\text{vesicle}}^2) \right] = 405000$ with $r_{\text{vesicles}} = 50 \text{ nm}$.

References

- [1] W. Rasband, *ImageJ* (<http://imagej.nih.gov/ij/>), <http://imagej.nih.gov/ij/>, 1997 - 2011.
- [2] E. Reimhult, M. Zach, F. Hook and B. Kasemo, *Langmuir*, 2006, **22**, 3313–3319.
- [3] S. Kaufmann, G. Papastavrou, K. Kumar, M. Textor and E. Reimhult, *Soft Matter*, 2009, **5**, 2804 – 2814.
- [4] S. Kaufmann, O. Borisov, M. Textor and E. Reimhult, submitted.